The hydroxyl species and acid sites on diatomite surface: a combined IR and Raman study

P. Yuan[a,*], D.Q. Wu[a], H.P. He[a], Z.Y. Lin[b]

[a]*Guangzhou Institute of Geochemistry, Chinese Academy of Sciences, Guangzhou 510640, China*
[b]*State Key Laboratory for Physical Chemistry of Solid Surfaces, College of Chemistry and Chemical Engineering, Xiamen University, Xiamen 361005, China*

Abstract

Diffuse reflectance infrared Fourier transform spectroscopy (DRIFT), Raman spectroscopy of adsorbed pyridine molecules (Py-Raman) and in situ Py-IR have been used to investigate the hydroxyl species and acid sites on diatomite surfaces. The Lewis (L) and Brønsted (B) acid sites, and various hydroxyl species, including isolated hydroxyl groups, H-bonded hydroxyl groups and physically adsorbed water, are identified. The L acid sites in diatomite samples are resulted from the clay impurities, and the B acid sites are resulted from some moderate strength H-bonded hydroxyl groups. At room temperature, both of the isolated and H-bonded silanols associate with the physically adsorbed water by hydrogen bond. After calcination treatment, physically adsorbed water will be desorbed from the silanols, and the silanols will condense with the increase of temperature. Generally, the H-bonded silanols condense more easily than the isolated ones. The properties of surface hydroxyl species of diatomaceous silica are more similar to precipitated silica rather than fumed silica.
© 2003 Elsevier B.V. All rights reserved.

1. Introduction

Diatomite is a kind of mineral assemblage in natural sediments. It consists of frustule, the silicified hard shell of diatom, and some other minerals such as clay minerals and feldspar, etc. [1]. The diatom shell, which is composed of amorphous silica, has properties such as high porosity with strong adsorbability and excellent thermal resistance. Hence, diatomite has been widely used as filter aid, catalytic support, and adsorbent [2–4]. Recently, the novel applications of diatomite as biological support, pharmic carrier, chromatogram support, and functional filler have attracted extensive attentions [5,6].

Similar to synthetic amorphous silicas, the reactivity of diatomite intrinsically links to the presence of reactive sites on their surface. Reactive sites not only condition the charge, acidity, solubility, and hydrophilicity of the surface, but they are also the sites of grafting and ligand-exchange reactions [7], so that they govern the properties of related diatomite products to great extent. To better understand and control

* Corresponding author. Tel.: +86-20-85290341;
fax: +86-20-85290130.
E-mail address: yuanpeng@gig.ac.cn (P. Yuan).

the properties of diatomite, it is important to have detailed information of the reactive sites.

Generally, the hydroxyl groups are primary reactive sites on the surface of amorphous silica (for comprehensive reviews, see Iler [8] and Bergna [9]). According to previous studies on synthetic amorphous silica by MAS NMR and IR [7–11], surface hydroxyl groups have been classified based on their coordination (single and geminal hydroxyl groups bonded to a $^3Q(OH)$ or $^2Q(2OH)$ silicon, respectively) and their hydrogen bonding (isolated and H-bonded hydroxyl groups). To the best of our knowledge, however, the surface hydroxyl species of diatomaceous silica have not yet been systematically investigated.

Besides hydroxyl groups, acid sites have been also thought as important surface sites of diatomite. Using Py-IR spectroscopy, Yang et al. [12] proved the existence of both Brønsted (B) and Lewis (L) acid sites in diatomite samples from Zhejiang province, China. Nevertheless, further study about the properties, origins and intensities of the acid sites has not been developed.

IR spectroscopy has proved to be a powerful method to identify the isolated and H-bonded hydroxyl groups on the surface of synthetic silica [8,9]. However, Wang and Zhang [1] did not successfully detect hydroxyl groups on diatomite surface using transmission infrared spectroscopy. Frost and Johansson [13] proposed that diffuse reflectance infrared Fourier transform spectroscopy (DRIFT) is more applicable than transmission infrared spectroscopy for powder samples because it provides a rapid technique for analyzing samples without any interference through sample preparation, and the technique is particularly suitable for the study on the hydroxyl stretching region of silicate minerals.

In this work, the DRIFT was used to investigate the hydroxyl species on diatomite surface. The surface acidities of diatomite, including the type, origin, intensity of acid sites, were studied by Raman spectroscopy using pyridine (Py) as probe molecule (Py-Raman), and an in situ Py-IR method was used as a complementary method.

2. Materials and methods

Diatomite samples, collected from Buchang deposit in Haikang county of Guangdong province, and Yuanjiawan deposit in Shengxian county of Zhejiang province, China, are denoted as BR and YR, respectively. After purification by repeated sedimentation and desiccation at 105 °C, the samples were grounded to less than 40 μm in mortar and kept in desiccator. The purification method of acid washing that has proved effective [2,14] was avoided to prevent the sample surface from possible disturbance or reconstruction. The purified samples are denoted as BP and YP, respectively.

A variable-temperature thermal treatment was conducted, with combination of the spectroscopy method, to investigate the properties of surface sites. The phase transformation of diatom shell, in which diatomaceous silica crystallized from disordered opal to ordered 'α-cristobalite, has proved at ca. 1150 °C for Buchang diatomite sample and at 1100 °C for Yuanjiawan sample by previous studies [1,15] and confirmed by this work. Accordingly, the thermal treatment was performed with the temperature range of 200–1100 °C in the present study. A corundum pot with about 500 mg diatomite was placed in a programmed temperature-controlled muffle oven for treatment. The samples were heated from room temperature to appointed temperature at a rate of 5 °C/min, and kept at the temperature for 1 h. The room temperature (RT) is at 23 ± 1 °C, and the relative humidity is about 70%.

The X-ray diffraction patterns of the samples were performed with a D/max-1200 diffractometer with Cu Kα radiation under target voltage 40 kV and current 30 mA in a scanning rate of $5°\ 2\theta$/min. The micromorphology of sample was observed under Hitachi S-3500N scanning electron microscopy (SEM). The specific surface areas of samples were performed with a NOVA-1000 apparatus using nitrogen as adsorbate (BET method).

A Nicolet 740 Fourier transform infrared spectrometer with a diffuse reflectance attachment was used to measure the DRIFT spectra over 160 scans at a resolution of 4 cm^{-1}. Sample powder was lightly packed into a 8-mm inter diameter microsample cup for experiment. The reflectance spectra of samples were ratioed against an Al mirror background reference. H_2O and CO_2 were purged by nitrogen from the attachment before experiment. A pure kaolinite sample from Suzhou, China, was used as a reference sample.

The Py-Raman study was performed with a confocal microprobe Raman system (LabRaman I, Dilor SA). The excitation line was 632.8 nm from a He–Ne laser and the spectra were recorded over 60 scans at a resolution of 2 cm^{-1}. Sample powder was pressed into a self-supported disk with a diameter of about 10 mm. Two drops of Py liquids were dropped to wet the disk surface, and the wet disk was quickly transferred onto the specimen stage for taking spectra.

The in situ Py-IR spectra were recorded on a Perkin-Elmer Spectrum 2000 system equipped with a liquid-nitrogen-cooled MCT detector and a home-built transmittance IR cell designed to treat the sample in situ. Sample was pressed into a self-supported disk with a diameter of about 10 mm. Before the introduction of Py, the sample disk was treated in the IR cell at 500 °C for 30 min and then evacuated (10^{-3} Torr) at the same temperature for more than 5 h, until surface contaminants such as carbonates species were completely removed. All of the reported absorbance was obtained from spectra referenced to the background spectra, which were taken under vacuum prior to the introduction of Py. The spectra were recorded over 36 scans at a resolution of 4 cm^{-1}.

3. Results

3.1. SEM and chemical analysis

The SEM result shows that most of diatoms in sample BR belong to the genera *Synedra ulna* (Nitz.) Ehr., with short diameter of 3–15 µm, and long diameter of 40–120 µm. Most of diatoms in sample YR belong to the genera *Melasira granulata* (Ehr.) Ralfs., with diameter of 10–30 µm.

The mineralogical compositions (shown in Table 1) of the four samples, evaluated by their XRD patterns, show that there are only small quantities of quartz and kaolinite impurities in sample BP while sample YP contains considerable quartz and clay impurities after sedimentation. This is consistent with that shown by chemical analysis. As shown in Table 2, sample YP contains more Al_2O_3 than sample BP, which results from clay mineral impurities.

3.2. DRIFT

Fig. 1 shows the DRIFT spectra of samples treated at different temperatures. Spectrum a, corresponding to sample BR exposed at room temperature for 24 h,

Table 1
Mineralogical compositions of diatomite samples (wt.%)

	Diatom shell	Quartz	Kaolinite	Montmorillonite	Illite	Mica	Feldspar	Other impurities
BR	78.6	5.4	7.9			3.3	2.9	1.9
BP	93.2	1.0	4.8					1.0
YR	59.5	11.9	8.2	6.8	5.4	4.3	1.5	2.4
YP	80.0	4.9	5.3	3.3	2.0	3.0		1.5

Table 2
Chemical compositions of diatomite samples (wt.%)

	SiO_2	Al_2O_3	Fe_2O_3	CaO	MgO	K_2O	Na_2O	TiO_2	MnO_2	Lost	Total	Sa[a] (m^2/g)
BR	82.95	5.75	1.41	0.24	0.21	0.06	0.06	0.69		7.93	99.30	14.0
BP	84.13	1.93	0.72							10.72	97.50	30.9
YR	65.24	15.96	3.12	0.50	1.66	1.17	0.29	0.56	0.01	10.46	99.51	11.8
YP	74.52	9.64	1.33							9.78	95.27	23.1

[a] SA: specific area.

Fig. 1. DRIFT spectra of diatomite samples.

displays one broad band centered at ca. $3500 \, cm^{-1}$ and three bands at 3694, 3661, and $3622 \, cm^{-1}$, respectively. After treatment at 200 °C, a shoulder band at $3739 \, cm^{-1}$ appears (Fig. 1b) and the intensity of the broad band decreases obviously while those of the other three ones remain unchanged.

The 3694, 3661, and $3622 \, cm^{-1}$ bands (Fig. 1a–e) should be attributed to the OH vibration mode of hydroxyl groups of kaolinite impurity because their positions are very consistent with those in the IR spectrum reported [16] and the kaolinite reference in this work (Fig. 1h).

The broad band centered at $3500 \, cm^{-1}$, whose intensity decreases with the increase of temperature and finally disappears at 1000 °C, should be attributed to OH vibration mode of the physically adsorbed H_2O.

The $3739 \, cm^{-1}$ shoulder band becomes more intense after calcination at 650 °C (Fig. 1d). The band is obviously asymmetric toward lower wavenumber. Its intensity increases after treatment at 650 °C and reaches its maximum at 1000 °C (Fig. 1e and f) with a higher wavenumber of $3745 \, cm^{-1}$. At 1100 °C (Fig. 1g), the band shifts to a lower wavenumber at

$3740 \, cm^{-1}$, with the increase of symmetry and obvious decrease of intensity.

The $3739 \, cm^{-1}$ shoulder band should be attributed to OH vibration mode of H-bonded hydroxyl groups that has been reported at about $3740 \, cm^{-1}$ [17]. At the same time, the isolated hydroxyl groups may contribute to the band because the bands of isolated hydroxyl groups are very close to the bands of H-bonded ones [9,17,18]. It shows that most of the silanols on sample surface associate with H_2O at room temperature, so that their IR bands are poorly resolved. After thermal treatment, with desorption of water and the exposure of more silanols, the intensity of the bands increase.

With the increase of temperature from 200 to 1000 °C (Fig. 1b–f), the $3739 \, cm^{-1}$ band shifts to the higher wavenumber, reflecting that the H-bonded silanols condense gradually in the order of H bond strength. That is to say, the stronger the hydrogen bond is, more easily the condensation of the H-bonded silanols occurs [10,17,19,20].

After calcination at 1000 °C, the quantity of isolated silanols, which have IR bands at $3745 \, cm^{-1}$, reaches its maximum. Some survived H-bonded

silanols result in the band to be asymmetric by broadening it toward lower wavenumber. This reflects the condensation of isolated silanols is more difficult than the H-bonded ones. After treatment at 1100 °C, the intensity of 3745 cm^{-1} band decreases sharply (Fig. 1g), indicating that almost all isolated silanols have condensed.

The spectra of sample BP are similar to those of BR except the bands attributed to kaolinite are poorly resolved (Fig. 1i–k). On the contrary, in the spectra of sample YP, the bands of kaolinite are well resolved (Fig. 1l–n), and the silanols have completely condensed after treatment at 1100 °C (Fig. 1q). In the spectra of YP, unlike BR and BY, the intensity of band at 3745 cm^{-1}, assigned to the isolated hydroxyl group, reaches its maximum when temperature increases to

900 °C (Fig. 1o). After calcination at 1000 °C, the 3745 cm^{-1} band weakens sharply with its position remaining unchanged (Fig. 1p).

3.3. Py-Raman

At room temperature and at 200 °C, the Py-Raman spectra only show two strong bands at 991 and 1031 cm^{-1} (Fig. 2a and b). The two bands are attributed to the U_1 and U_{12} modes of ring-breathing vibrations (UCCN) of liquid Py [21,22]. After calcination at 400 °C, a weak shoulder band at 998 cm^{-1} appears (Fig. 2c). After treatment at 650 °C it becomes more intense, and a weak 1016 cm^{-1} band appears (Fig. 2d). The 1016 cm^{-1} band is very weak in the spectrum of BP (Fig. 2h). After calcination at 900 °C,
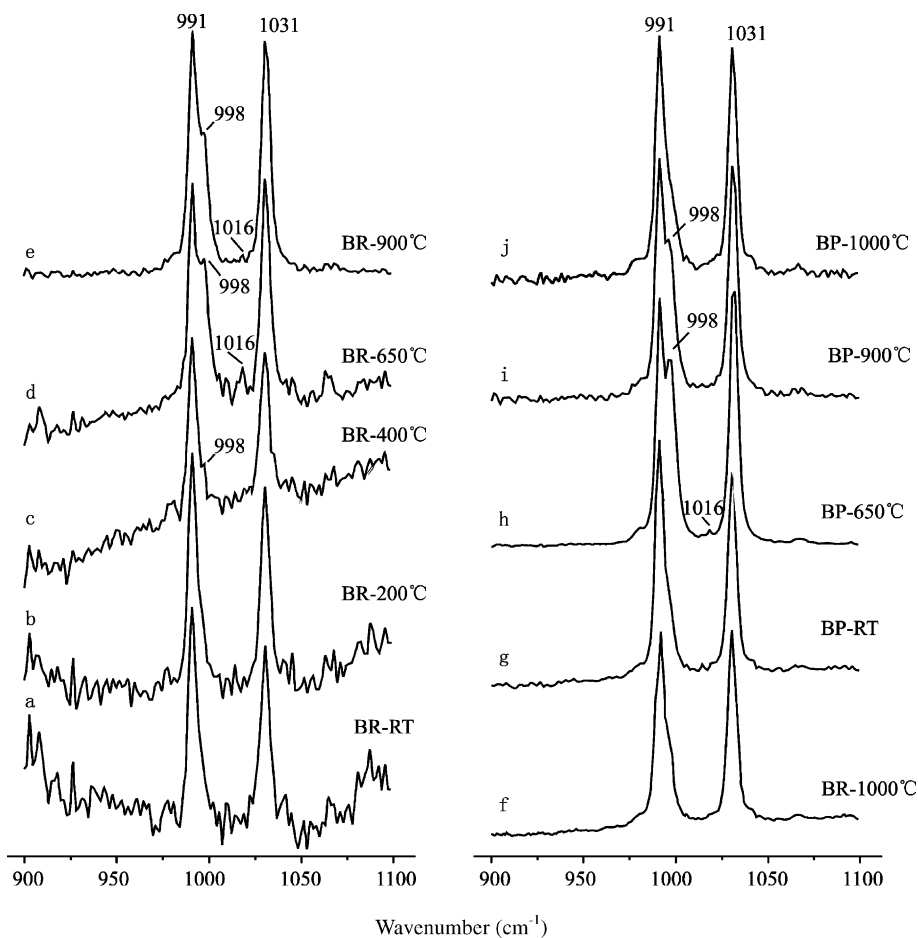
Fig. 2. Py-Raman spectra of BR and BP under thermal treatment conditions.
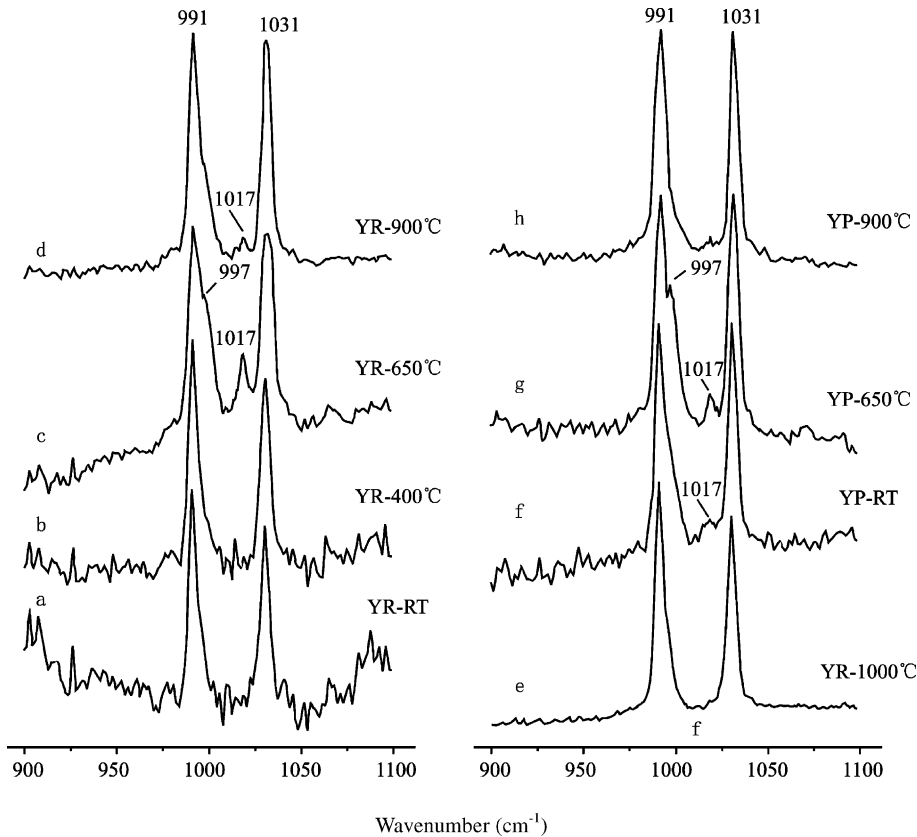
Fig. 3. Py-Raman spectra of YR and YP under thermal treatment conditions.

the intensity of the 998 cm^{-1} band decreases obviously. The 1016 cm^{-1} band becomes very weak in the spectrum of BR, and disappears in the spectrum of BY (Fig. 2e and i). After treatment at 1000 °C, there are no bands well resolved except the 991 and 1031 cm^{-1} bands (Fig. 2f and j).

The band at 998 cm^{-1} should be attributed to the U_1 mode of ring-breathing vibration (UCCN) of PyH$^+$, resulting from the Py associating with the proton (H$^+$) released by B acid sites; and the 1016 cm^{-1} band should be attributed to the U_1 mode of ring-breathing vibration (UCCN) of LPy, resulting from Py coordinating to L acid sites [21,22]. Hence, the two bands reflect the existance of both B and L acid sites in diatomite samples.

The Py-Raman spectra of YR and YP are similar to those of BR and BY (Fig. 3). However, under the same thermal treatment condition, the intensities of the bands at 1017 cm^{-1} corresponding to L acid sites are always stronger than that in the spectra of BR and BY (Fig. 2).

3.4. In situ Py-IR

For in situ Py-IR, the sample BR and BY treated at 650 °C are used in the present study since they bear relatively abundant acid sites, proved by the Py-Raman analysis. In the spectrum of BR evacuated at 50 °C, there are two strong bands at 1445 and 1596 cm^{-1}, two weak bands at 1580 and 1541 cm^{-1} and a negative absorbance at 3744 cm^{-1} (Fig. 4a).

The assignments of the above bands should be as follows [23]: 1445 cm^{-1}, the v_{19b} mode of ring-breathing vibration (vCCN) of PyH$^+$; 1541 cm^{-1}, the v_{19b} mode of ring-breathing vibration (vCCN) of LPy; 1580 and 1596 cm^{-1}, the v_{8a} vibration modes (vCCN) of Py H-bonded with surface. Accordingly, it shows that there are considerable L acid sites in the
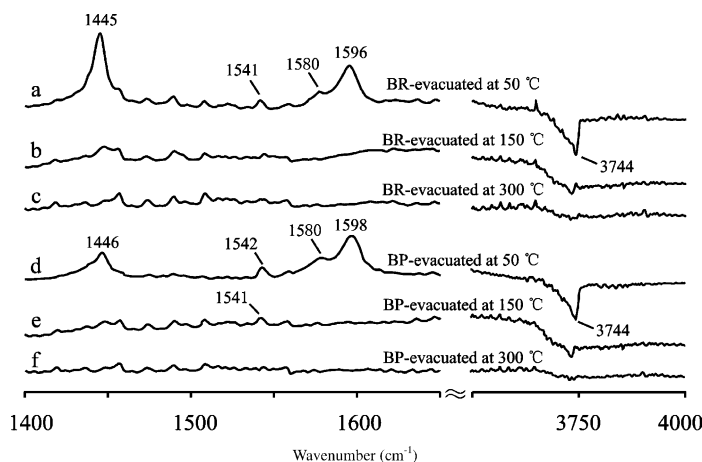
Fig. 4. In situ Py-IR spectra of diatomite samples.

sample BR heated at 650 °C. However, the quantity of B acid sites is limited, and most of Py molecules are adsorbed on the surface by hydrogen bond.

The negative band at $3744 \, cm^{-1}$ indicates that the hydroxyl groups have reacted with Py in some way [23,24]. Coincident with this, the $1596 \, cm^{-1}$ band to the vibration mode of Py H-bonded with surface is very strong, while the $1541 \, cm^{-1}$ band to the vibration mode of PyH^+ is weak. This indicates that adsorption of most of Py on diatomite essentially via H-bonding to hydroxyl groups.

After evacuation at 150 °C, the intensities of all the bands decrease sharply (Fig. 4b). The 1580 and $1596 \, cm^{-1}$ bands become too weak to be resolved, indicating that H-bonded Py have been desorbed completely. At the same time, the significant decrease of 1445 and $1541 \, cm^{-1}$ bands shows that most Py molecules have been desorbed from their association with L and B acid sites. After evacuation at 300 °C, there are no bands well resolved (Fig. 4c).

The spectra of BY (Fig. 4d–f) are very similar to those of BR. However, after evacuation at 150 °C, the $1542 \, cm^{-1}$ band still exists with decrease of intensity.

4. Discussion

4.1. Surface hydroxyl species

The results of previous IR studies about the silanols of synthetic silica, including the pyrogenic silica, the precipitated silica and quartz, could be summarized as follows [17–19,25]: (1) The band corresponding to isolated hydroxyl group is in the range of 3745–$3750 \, cm^{-1}$, and variations might result from different treatment conditions and various types of silica. The band of H-bonded hydroxyl group is at about $3740 \, cm^{-1}$, and sometimes combines with the band of isolated hydroxyl group to form a single asymmetric band when the instrument lacks enough resolving power. (2) With the increase of treatment temperature, the silica would experience a process of desorption of water and condensation of silanols. Isolated silanols are more difficult to condense than H-bonded ones and their condensation temperature varies with the type of silica and treatment conditions. The condensation of H-bonded silanols occurs by the order of strength of hydrogen bond: the stronger the hydrogen bond is, the more easily the condensation occurs.

Based on the spectra of sample BR, scheme I–V (Fig. 5) is assumed to elucidate the hydroxyl structure and the dehydration process of diatomaceous silica.

There are two types of silanols, isolated and H-bonded silanols, on diatomite surface (Fig. 5). At room temperature, both of the two types of silanols are H-bonded with water. Consequently, there are no well-resolved bands of the silanols in the DRIFT spectrum except the broad band of H_2O at $3500 \, cm^{-1}$. With the increase of temperature of 200–1000 °C, five dehydration processes are assumed, shown as scheme I–IV in Fig. 5. At first, the desorption of water results in the
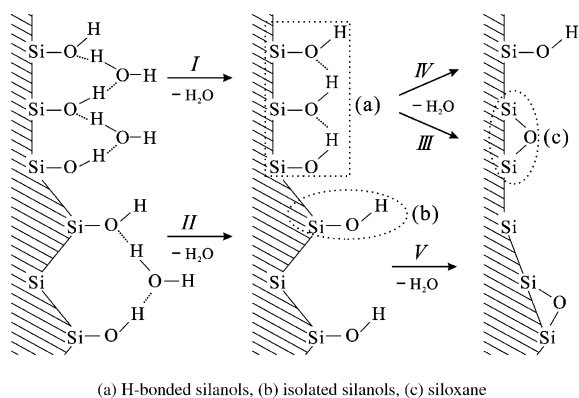
(a) H-bonded silanols, (b) isolated silanols, (c) siloxane

Fig. 5. The hydroxyl structure and the dehydration process of diatomaceous silica.

decrease of intensity of the H_2O band and the appearance of the 3739 cm^{-1} shoulder band corresponding to the silanols (Fig. 5, I and II). With continuous desorption of water and the exposure of more and more silanols, the band becomes stronger and stronger with position progressively moving to higher wavenumber, and near the position of band corresponding to isolated silanol. This reflects that some strongly H-bonded silanols begin to condense to form siloxane bridges (Fig. 5, scheme III and IV) while most of the isolated silanols have not condensed. This shows that for the H-bonded silanol in diatomaceous silica, the weaker the hydrogen bond is, the closer its band nears that of isolated silanol, and more difficult the occurrence of condensation is. At 1000 °C, the intensity of 3745 cm^{-1} band reaches its maximum, indicating the amount of isolated silanols reaches the maximum. The asymmetry of this band toward the lower wavenumber reflects that there are some weakly H-bonded silanols remain on the surface.

At 1100 °C, most of isolated silanols condense as shown in scheme V. The condensation temperature of isolated silanols in this study is higher than the synthetic silicas reported. This may result from different treatment condition, under which a heat process only for 1 h is used in the present study, while in previous works evacuation and calcination process beyond 6 h are applied [10,17].

The residual weak band at 3740 cm^{-1} reflects the existence of a few H-bonded silanols. As for silica with micropore or mesopore structure, Bogdan et al. [26] proposed that the hydroxyl groups exist on the inner wall of pores arrange closely and prefer to form H-bonded hydroxyl groups, and the condensation temperature of them is generally high. The sample BR contains mesopores with diameter of 10–20 nm [15], so it can be presumed that most of the survival Hhydrogen-bonded silanols remain in these mesopores after treatment at 1100 °C. The strong thermal resistance of these silanols might result from the shielding of mesopore frameworks.

Unlike BR and BP, the position of band at 3745 cm^{-1} remains unchanged despite of the decrease of its intensity in the spectrum of YP after calcination at 1000 °C, which may result from the lack of mesopores in sample YP. Yang et al. [15] found that the sample YR only contains a macropore structure with diameter of 115–147 nm. This can be taken as an evidence for the above assumption that the residual H-bonded hydroxyl groups remain in the mesopores for BR and BP.

As shown by DRIFT, the silanols of BR and BP have relatively higher condensation temperature than those of YP. Also, the phase transformation temperature of YR is found to be lower than BR [12,15], which has been ascribed to the stronger thermal resistance of the *S. ulna* (Nitz.) Ehr. than the *M. granulata* (Ehr.) Ralfs. Actually, because the influence of impurities on the thermally resistant ability has proved considerable [27], the impurities should be thought as another important factor to affect the thermal resistance of the diatomite, besides the factor of genera. It may be more meaningful if we can take pure cultivated diatom as sample in future work.

Compared with precipitated silica and pyrogenic silica [9,17–19,25,27], the properties of surface silanols in diatomaceous silica are more similar to precipitated silica than to pyrogenic silica. Just like the silanols in precipitated silica, the silanols in diatomaceous silica are shown to be predominately hydrogen bonded at room temperature, while those in Cab–O–Sil, a pyrogenic silica, are shown to be both isolated and H-bonded [10].

Differences among the silicas are probably resulted from the formation conditions. McDonald proposed that the Cab–O–Sil is formed at high temperature, so the rate of rearrangement of silica tetrahedral must be greater than that of precipitated silica, which is formed in solution [17]. Since configurations with local ordered resembling that in the crystal must be more

stable than disordered configurations, the silica tetrahedral tends to rearrange to the more ordered configurations. As a consequence, a larger fraction of surface silanols of Cab–O–Sil is well separated [17]. However, Liu and Maciel [10] assumed that some surface silanols, trapped at the contact point between two or more silica globules obtained during the process of aggregation, are isolated silanols because they have little chance to be accessible by water molecules by reason of steric hindrance.

The geminal silanols are difficult to be distinguished from the isolated ones in spectra of IR since the bands of them are too close to be well resolved [9]. Our work based on the ^1H–^{29}Si CP/MAS NMR, proved to be a powerful method to identify the geminal silanols [28], will be reported in the following paper.

4.2. L and B acid sites

The results of Py-Raman and in situ Py-IR on acidity show that there are no acid sites detected in samples before thermal treatment. After calcination at 650 °C, the quantity of B and L acid sites reaches their maxima. Under the same thermal treatment condition, the L acid sites in raw samples are more abundant than in the purified ones, and the L acid sites in the series of YP are more abundant than the corresponding BP ones.

Obviously, the quantity of L acid sites is strongly affected by the temperature of thermal treatment, and positively relates to the content of clay impurities in diatomite sample. For the BP, in which clay impurities has been completely removed, the quantity of L acid sites is very limited even after treatment at 650 °C.

Thus, we propose that the L acid sites mainly resulted from clay mineral impurities in diatomite. For the 2:1 type clay such as montmorillonite, vermiculite, mica, etc., Al^{3+} proxying for Si^{4+} in tetrahedral coordination in an aluminosilicate gives rise to a net negative charge. A H_3O^+ would associate with such tetrahedral aluminum to balance charge. It corresponds to a B or protonic acid site. Aluminium in three-fold coordination, perhaps occurring at an edge, or arising from a dehydroxylation of the B site after calcination, would correspond to the L acid site [29]. For the 1:1 type clay such as kaolinite, an octahedral Al^{3+} that located at a platelet edge will function as

L acid site after dehydration [30]. The origins of the acid sites and its mechanism in clay minerals under calcination treatment have been discussed in detail in previous reports [29,30].

There are two possible origins of the B acid site in the diatomite: one is the hydroxyl group; another one is the charge-balancing H_3O^+ in 2:1 type clay mineral impurities as discussed above. In the case of pure diatomite sample, the B acid sites resulted from impurities will be few, and the hydroxyl groups are the primary origin of B acid sites. According to the Py-Raman results, the quantity of B acid sites reaches the maximum after calcination at 650 °C. At 1000 °C, most of the B acid sites are lost. However, at the same temperature, the quantity of isolated hydroxyl groups reaches its maximum. This shows that most of the isolated hydroxyl groups do not play the role of B acid sites, while some H-bonded hydroxyl groups, most of which has not yet condensed until calcination at 1000 °C, should be the main origin of B acid sites.

Roughly, we can classify the H-bonded hydroxyl groups as strongly H-bonded hydroxyl groups, whose condensation temperature is below 650 °C, moderate strength H-bonded hydroxyl groups, whose condensation temperature is in the range of 650–1000 °C, and weakly ones, whose condensation temperature is beyond 1000 °C. Then the moderate strength H-bonded hydroxyl groups should be the main origin of B acid sites. The strength of both B and L acid sites is weak since the coordination of PyH^+ and LPy is mostly destroyed after evacuation at 150 °C.

5. Conclusions

A model is proposed to elucidate the hydroxyl structure and the dehydration process of diatomite. At room temperature, both the isolated and H-bonded hydroxyl groups on the surface of diatomaceous silica are H-bonded with physically adsorbed water. After calcination treatment, physically adsorbed water will be driven away from the surface, and the hydroxyl groups will condense. The H-bonded hydroxyl groups condense more easily than the isolated ones. The stronger the hydrogen bond is, the more easily condensation occurs. Basically, the properties of surface hydroxyl species of diatomaceous silica are more similar to precipitated silica than to fumed silica.

The variety of condensation temperature of silanols in diatomite samples is resulted from the content of impurities, and the difference of thermal resistance among various diatoms.

Both the Lewis and the Brønsted acid sites in diatomite are weak. The L acid sites are resulted from clay mineral impurities. The B acid sites resulted from some moderate strength H-bonded hydroxyl groups, whose condensation temperature is in the range of 650–1000 °C, and the quantity of them is small.

Acknowledgements

References

[1] F.Y. Wang, H.F. Zhang, Chin. J. Geochem. 14 (1995) 140.
[2] E. Galán, I. González, E. Mayoral, A. Miras, Appl. Clay Sci. 8 (1993) 1.
[3] B. Erdogan, S. Demirci, Y. Akay, Appl. Clay Sci. 11 (1996) 55.
[4] P.V. Vasconcelos, J.A. Labrincha, J.M.F. Ferreira, J. Eur. Ceram. Soc. 20 (2000) 201.
[5] X. Wang, S. Gao, L. Yu, C. Miao, Chem. J. Chin. Univ. (in Chinese) 19 (1998) 854.
[6] X. Li, C. Bian, W. Chen, J. He, Appl. Surf. Sci. 207 (2003) 378.
[7] J.B. Caillerie, M.R. Aimeur, Y.E. Kortobi, A.P. Legrand, J. Coll. Interface Sci. 194 (1997) 434.
[8] R.K. Iler, The Chemistry of Silica, Wiley, New York, 1979.
[9] H.E. Bergna, Colloid chemistry of silica: an overview, in: H.E. Bergna (Ed.), The Colloid Chemistry of Silica, American Chemical Society, 1994.
[10] C.C. Liu, G.E. Maciel, J. Am. Chem. Soc. 118 (1996) 5103.
[11] T. Takei, K. Kato, A. Meguro, M. Chikazawa, Coll. Surf. A: Physicochem. Eng. Aspects 1590 (1999) 77.
[12] Y. Yang, J. Wu, P. Wang, J. Inorg. Chem. (in Chinese) 12 (1996) 356.
[13] R.L. Frost, U. Johansson, Clays Clay Miner. 46 (1998) 466.
[14] N. Videnov, S. Shoumkov, Z. Dimitrov, L. Mogilski, L. Brakalov, Int. J. Miner. Process. 39 (1993) 291.
[15] Y.X. Yang, R.S. Chen, A.B. Dai, Acta Chimica Sinica (in Chinese) 54 (1996) 57.
[16] V.C. Farmer, Clay Miner. 33 (1998) 601.
[17] R.S. McDonald, J. Phys. Chem. 62 (1958) 1168.
[18] B.A. Morrow, A.J. Mcfarian, J. Non-Cryst. Solids 120 (1990) 61.
[19] B.A. Morrow, A.J. Mcfarian, J. Am. Chem. Soc. 96 (1992) 1395.
[20] C.E. Bronnimann, R.C. Zeigler, G.E. Maciel, J. Am. Chem. Soc. 110 (1988) 2023.
[21] E. Payen, M.C. Dhamelincourt, P. Dhamelincourt, Appl. Spectrosc. 36 (1982) 30.
[22] M.I. Zaki, A.A.M. Ali, Coll. Surf. A: Physicochem. Eng. Aspects 119 (1996) 39.
[23] M.I. Zaki, M.A. Hasan, F.A.A. Sagheer, L. Pasupulety, Coll. Surf. A: Physicochem. Eng. Aspects 190 (2001) 261.
[24] M.W. Urban, Vibrational Spectroscopy of Molecules and Macromolecules on Surfaces, Wiley, Chichester, 1993.
[25] D.A. Koretsky, J.W. Sverjensky, J.W. Salisbury, Geochim.t Cosmochim. Acta 61 (1997) 2193.
[26] A. Bogdan, M. Kulmala, B. Gorbunov, J. Coll. Interface Sci. 177 (1996) 79.
[27] A. Djemai, E. Balan, G. Morin, J. Am. Ceram. Soc. 84 (2001) 1017.
[28] B. Humbert, J. Non-Cryst. Solids 191 (1995) 29.
[29] J.J. Fripiat, A. Leonard, J.B. Uytterhoeven, J. Phys. Chem. 69 (1965) 3274.
[30] D.H. Solomon, M.J. Rosser, J. Appl. Polym. Sci. 9 (1965) 1261.